Infrared Physics & Technology 133 (2023) 104801

Contents lists available at ScienceDirect

Infrared Physics and Technology

journal homepage: www.elsevier.com/locate/infrared

Fabrication of infrared detector with monolithic microlens produced in thermal reflow process

J. Chrzanowska-Giżyńska [a,b,*], O. Ślęzak [a,c], P. Nyga [a,d], M. Wankiewicz [a]

[a] VIGO Photonics, Poznańska 129/133, 05-850 Ożarów Mazowiecki, Poland
[b] Institute of Fundamental Technological Research, Polish Academy of Sciences, Pawińskiego 5B, 02-106 Warsaw, Poland
[c] Faculty of Advanced Technologies and Chemistry, Military University of Technology, gen. Sylwestra Kaliskiego 2, 00-908 Warsaw, Poland
[d] Institute of Optoelectronics, Military University of Technology, gen. Sylwestra Kaliskiego 2, 00-908 Warsaw, Poland

ARTICLE INFO

Keywords:
Microlens
Thermal reflow
InAsSb
MBE
Infrared detector
Detectivity
III-V detector

ABSTRACT

We report fabrication of monolithic GaAs immersion lens with a sub-milimeter diameter for InAsSb infrared detectors. The microlenses were produced by thermal reflow process of cylindrical photoresist structures, followed by dry etching. The implementation of microlens leads to an increase in the optical area of the photodetector, while maintaining the electrical area dimensions. Detectors with microlenses exhibit three times higher normalized detectivity D* than flat detectors, while conserving a similar level of resistance and current sensitivity. This result proves that the processes related to lens formation do not result in degradation of the photosensitive structure.

1. Introduction

An infrared detector is a semiconductor electronic device that finds applications in various fields such as temperature measurement systems, gas analysis, military tracking and detection system, people counting, and fire or smoke detection. The key parameters that define the usefulness of the detector are the intensity of current noise I_n, current sensitivity R_i, and spectral detectivity. While the sensitivity primarily depends on the parameters of the semiconductor photosensitive structure, current noise depends, among other factors, on the photosensitive surface area, as shown in the Equation (1).

$$I_n^2 = 2(N_G + N_R)At\Delta fq^2g^2 \tag{1}$$

where N_G and N_R represent the generation and recombination rates of charge carriers, A denotes the physical area of the photosensitive structure, t represents the thickness of the photosensitive structure, Δf denotes bandwidth, g is photoelectric gain, and q is electron charge.

This means that the detection of weak optical signals requires a detector with a small photosensitive area. Hence, applications that demand high sensitivity and large detection area typically employ multi-element detectors. However, the design of a flat multi-element detector can lead to distortion of the recorded signal due to optical crosstalk [1,2] and blind spots. An alternative solution is to use an immersion detector, which involves a monolithic integration of the detector element with a microlens. This increases the optical size of the detector relative to its physical size and results in a higher normalized detectivity D* by a factor of $(A_0/A)^{1/2}$, as shown in Equation (2).

$$D^* = \frac{1}{E}\left(\frac{A_0}{A}\right)^{\frac{1}{2}}\left(\frac{\eta}{t^{\frac{1}{2}}}\right)(2(N_G + N_R))^{-\frac{1}{2}} = \frac{R_i(A_0\Delta f)^{\frac{1}{2}}}{I_n} \tag{2}$$

Here, E represents photon energy, η represents quantum efficiency, R_i is current sensitivity and A_0 represents the optical surface area.

Immersion lenses for infrared detectors have been previously fabricated through a machining of back side surface of a wafer on which detector has been fabricated [3,4], or fabricated separately and attached to the back or front side of the detector using an optical contact method [5–7]. However, these solutions are expensive due to the need to process each workpiece separately, ensuring high centering and machining accuracy, and low processing temperature to avoid damage to the photosensitive structure. These factors contribute to the high cost and long production time of the detectors. To address this issue, we propose replacing the hyper-hemispherical lens with an integrated micro-lens produced through a thermal reflow technology followed by a dry etching. This proposed solution offers benefits such as the automation and parallelism of the production process, higher accuracy of manufactured elements and centering of lens and detector, reduction of

* Corresponding author.
E-mail address: jchrzanowska@vigo.com.pl (J. Chrzanowska-Giżyńska).

https://doi.org/10.1016/j.infrared.2023.104801
Received 27 April 2023; Received in revised form 19 June 2023; Accepted 22 June 2023
Available online 23 June 2023

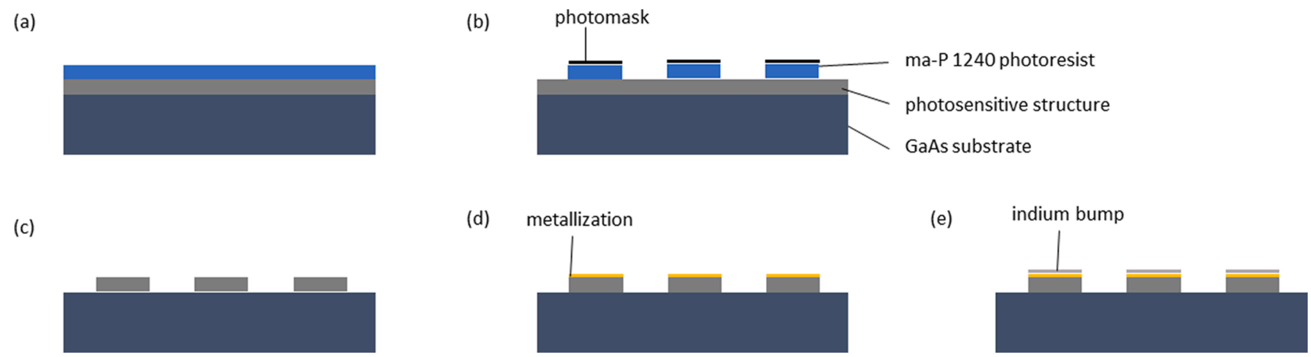

Fig. 1. Fabrication of InAsSb semiconductor mesa structure: (a) photoresist ma-P 1240 is spun on GaAs substrate, (b) photoresist structures are patterned, (c) InAsSb mesa is etched, (d) metallization is deposited, (e) indium bumps are deposited.

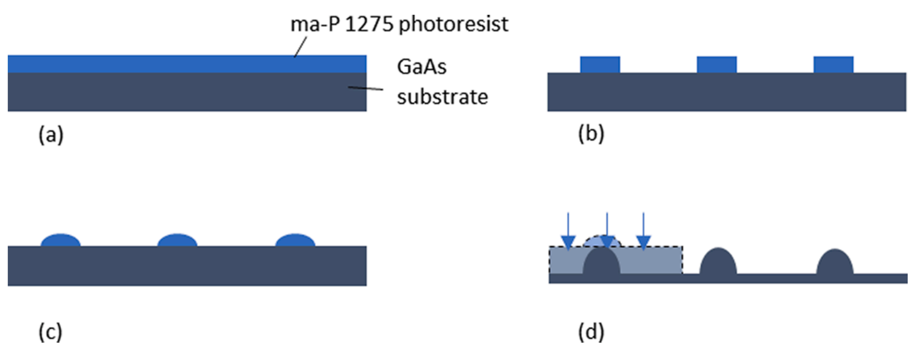

Fig. 2. Fabrication of GaAs lenses by thermal reflow and ICP etching: (a) photoresist ma-P 1275 is spun on GaAs substrate, (b) photoresist columns are patterned, (c) reflowed photoresist microlens, (d) plasma etched GaAs microlens.

manufacturing time, and thus a reduction in the unit cost.

Thermal reflow involves heating photoresist structures above the material's glass transition temperature to form a geometry with the lowest surface energy, i.e. a spherical shape. The profile of the photoresist after the reflow process depends on the temperature, heating time, photoresist volume, solvent content in the photoresist, as well as surface tension between photoresist and the substrate [8]. The larger the target diameter of the photoresist structure, the higher the initial photoresist structure thickness has to be. Thermal reflow process is well established for the production of small lenses [8,9] but fabrication of large tall and uniform structures is technologically difficult due to low homogeneity.

Micro lenses produced in the thermal reflow process are widely used in applications related to the analysis of visible and near infrared radiation, mainly using fused silica [9,10], silicon [11] and polymeric lenses [12,13]. However, processing micro-lenses for mid and far-infrared detectors is much more demanding because it requires other materials, mainly gallium arsenide. Moreover, in the case of immersion lenses manufacturing on the backside of a wafer with detecting structures already fabricated on the front side, use of elevated temperatures processing is limited by a thermal stability of epitaxial structures or the stability of the metallic contacts, e. g. the indium melting point is 156.6 °C.

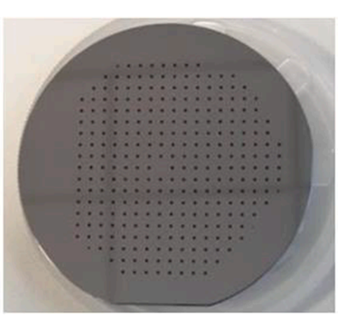

Fig. 3. Photoresist structures on the surface of 2'' GaAs wafer.

The goal of this work is to develop technology for lenses on the back side of a 2'' gallium arsenide wafer with InAsSb photosensitive structures. The position and geometry of the lenses were designed to increase the detectivity of the sensors by at least 2×, assuming the angle of view of the sensor to be 33.7°, the same as in the case of hyper hemispherical lens [4].

2. Materials and methods

2.1. Mesa structure processing

In this work, we considered the bulk InAsSb semiconductor mesa type detectors. We defined the pattern of mesa structures (100 μm × 100 μm) using maP-1240 positive tone photoresist from Micro Resist Technology GmbH. The structures were wet-etched. Next, the Pt/Ti /Pt/Au metallization with the use of negative tone photoresist was performed and indium bumps were deposited. Indium bumps are used for flip chip – interconnecting semiconductor structure and sapphire with metallized pads carrier. The process flow that was followed is presented in Fig. 1.

2.2. GaAs lens processing

The fabrication of microlenses in GaAs was achieved by resist reflow and inductively coupled plasma reactive ion etching (ICP-RIE). The GaAs substrate (AXT) is 2 in. in diameter and 1.1 mm thick. The process flow that was followed is presented in Fig. 2.

First, the maP-1275 photoresist (Micro Resist Technology GmbH) was spin-coated twice on the substrate at the speed of 1500 rpm for a

	Object Type	Comment
1	Source Ellipse ▾	
2	Ellipse ▾	scattering surface
3	Paraxial Lens ▾	external lens
4	Freeform Z ▾	immersion lens
5	Detector Rectangle ▾	photosensitive structure

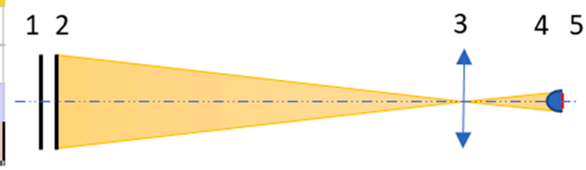

Fig. 4. Component order in Optic Studio (left) and optical layout of the analyzed system (right); not in scale.

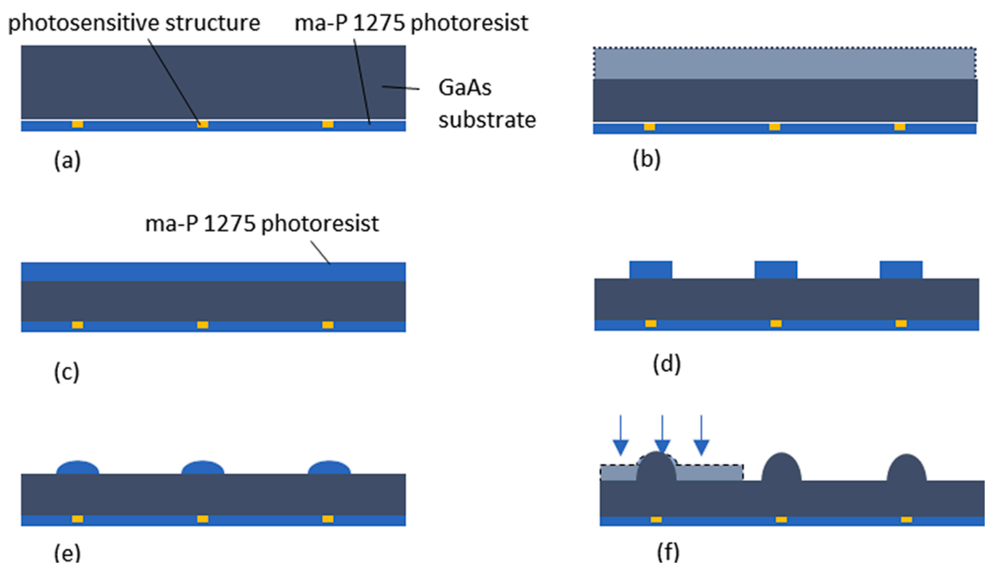

Fig. 5. Fabrication of an IR detector with an immersion lens involved several steps: (a) The mesa structures were protected by applying a layer of ma-P 1275 photoresist to prevent damage. (b) The thickness of the GaAs substrate was determined using a lapping and polishing system. (c) A photoresist, ma-P 1275, was spun onto the GaAs substrate. (d) Patterning of photoresist columns was performed. (e) The photoresist was reflowed to form microlenses. (f) Plasma etching was carried out to create GaAs microlenses.

time of 60 s. Each photoresist coating was subjected to soft baking at 115 °C for 10 min. The resist thickness prepared in this way was 22 ± 1 μm. Next the exposure of photoresist was performed using a mask aligner (SUSS MictoTec) with a Hg lamp. The photolithography mask allows to obtain circles with a diameter of 520 μm which are equidistant from each other in the × and y directions, with a distance of 2 mm between them, as shown in Fig. 3. The portion of the photoresist that was exposed to light was removed by the photoresist developer (0.2 M NaOH solution). Then, photoresist columns were transformed into semi-spherical shapes by thermal reflow process at a temperature of 150 °C for 30 min. using a furnace (Drying oven SLN 115, Pol-EKO aperture). An ICP-RIE (PlasmaPro 100 ICP 180, Oxford Instruments) was then used to etch the reflow lenses into the GaAs wafer. The Cl_2/Ar plasma was maintained at a gas flow ratio of 6/11 sccm, the ICP power was 700 W, and the RF power was 300 W for all etching processes. The Endpoint Detection monitor was used to control the completion of photoresist etching.

The geometry of the photoresist columns and lenses was measured using an optical profilometer (S-neox, SENSOFAR). Measurements were performed in the interference mode with the 10 × objective and in the confocal mode with the 20 × objective.

The cross-section profiles of the ICP-etched reflow lens were analyzed using Scanning Electron Microscope (SEM) (SU3800, Hitachi).

2.3. Infrared detector with immersion lens processing

The optimal distance between GaAs microlens and the 100x100 μm photosensitive structure was estimated using optical simulations in the Zemax (OpticStudio) software. The geometry of the fabricated immersion lens was recreated in Non-Sequential mode using Freeform Z object. The optimal distance between the top of the lens and the photosensitive structure was analyzed using Universal Plot - visualization of changing variables on Merit. The thickness of the substrate has been optimized so that the lens guarantees a maximum increase in D* for an acceptance angle of 2θ from 0 to 33.7°. To optimize the device for the aforementioned angle of view, a paraxial lens with f-number f/0.6 was inserted in front of it. The analyzed object was defined as a 'source ellipse' behind which there was a radiation scattering plane in the "importance sampling" configuration. The analyzed device was placed in a location ensuring illumination of the entire optical surface of the immersion lens. The component order and optical layout of the analyzed system is presented in Fig. 4.

To ensure the optimal distance between the GaAs microlens and the photosensitive structure, after processing the mesa structure, the thickness of the GaAs substrate was defined using a lapping and polishing system (Logitech PM6). The wafer prepared in this way went through the lens manufacturing procedure, as shown in Fig. 5.

During the photolithography (Fig. 5 d) mask was centered in backside alignment mode so that the circles in the mask were centric to the mesa structures pattern. The centering accuracy was measured at the cross-section of the structure using the SEM. The offset of centering process was not greater than 5 μm.

2.4. Measurements of optical properties

Optical surface of the immersed detector was measured on a self-made scanning system presented in Fig. 6 To determine the relationship between the tilt of the mirror and the shift of the scanning spot, a calibration was performed before the measurements. Calibration consisted in performing a scan of a flat detector whose physical surface has

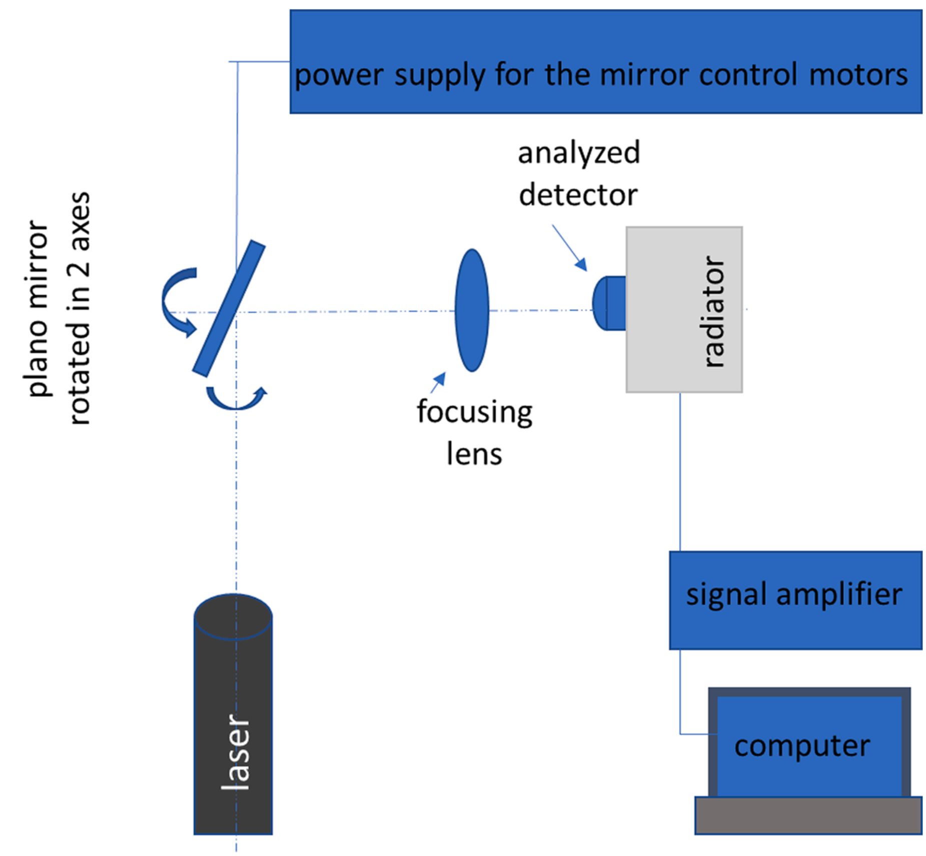

Fig. 6. Scanning system for determining the optical area of the immersed detector.

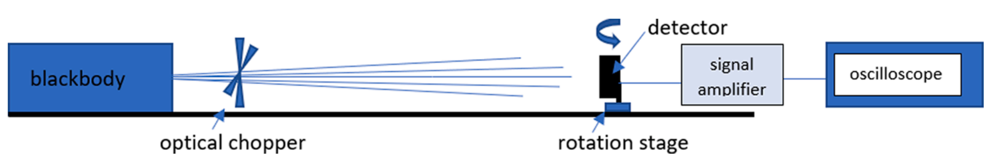

Fig. 7. The angle of view measuring position layout.

previously been measured using an optical microscope.

The angle of view was measured using a blackbody (BB) with a temperature of 1000 °C and an aperture of 10 mm. The detector with immersion lens was placed in front of blackbody at a distance of 1500 mm. The angular position of the detector relative to BB was controlled by a rotation stage in the range of ± 40°. This setup is illustrated in

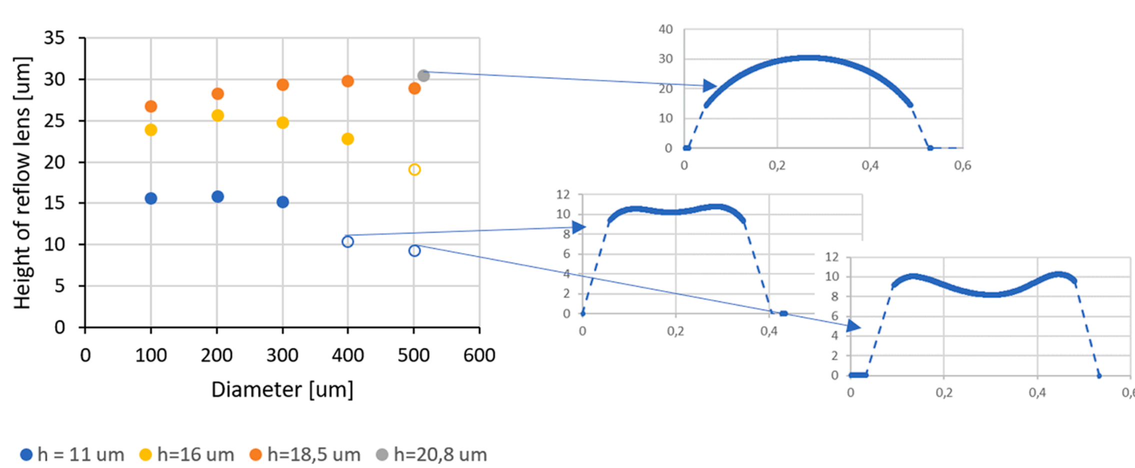

Fig. 8. Photoresist lens after the reflow process of the photoresist cylinder with a height of 11, 16, 18.5 and 20.8 um. Open circles represent a volcano like-shaped structure.

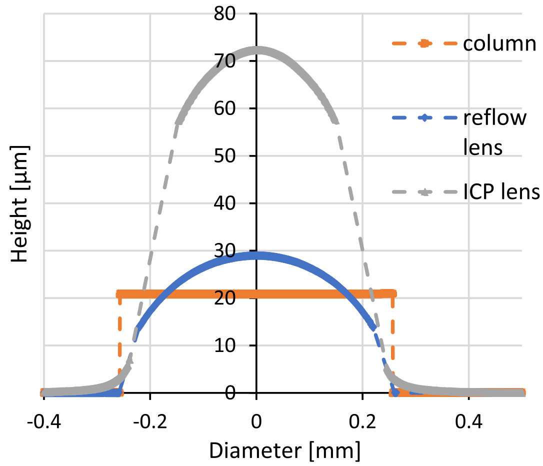

Fig. 9. Lens profile at various stages of manufacturing: photoresist column (orange), photoresist lens after reflow (blue) and GaAs lens after ICP etching (gray). The × and y scales are different. (For interpretation of the references to colour in this figure legend, the reader is referred to the web version of this article.)

Fig. 7.

2.5. Electrical properties

Measurements of the key electrical parameters of an immersed detector include resistance, current responsivity (R_i) and detectivity (D^*). The resistance was determined based on the I-V characteristic, while the current sensitivity was measured using FT-IR spectrophotometer (Perkin Elmer) with an external off-axis parabolic gold mirror. In the first stage of the measurement, the detector was positioned in the mirror's focal point, where the signal reached its maximum value, providing information on the detector's photocurrent per unit optical area [A/cm^2]. Next, a reference pyroelectric detector with a well-defined spectral characteristic was placed at the mirror's focal point to measure the pyroelectric detector's signal and thus determine the power of the source incident on the surface of pyroelectric detector [W/cm^2] for certain wavelength. R_i was defined as the quotient of the photocurrent from the detector and the source power.

3. Results and discussion

Previous literature reports [6] indicated that to create a photoresist structure with a spherical surface using a thermal reflow process, the minimum height of the photoresist column h is about 1/23 of its diameter φ. It depends on the surface tension of photoresist, the resist volume, and the diameter of the lens base during the melting step [6]. In this research the goal was to obtain homogeneous lenses on the entire surface of the 2'' GaAs wafer. Preliminary tests show that the maP-1275 photoresist allows to obtain homogeneous thickness (±0.5 µm) on a 2'' GaAs wafer up to 10.5 µm. Further tests show that spinning of ma-P1275 photoresist twice gives reproducible thickness equal to the sum of the thicknesses from individual spins.

The effect of photoresist thickness on the shape of the lens was tested for photoresist cylinders with diameters of 100, 200, 300, 400 and 500 µm. The tests indicate that the diameter of the column may be not more than 20 times the height of the photoresist. Otherwise, after the thermal reflow process photoresist lens collapses in the central part and creates a volcano like -shape structure, as shown in Fig. 8.

The ICP etching of the reflow lens was monitored with End Point Detection monitor to complete the etching after the photoresist was fully etched. Since the photoresist etch rate was about 70 nm/min and the GaAs etch rate was 160 nm/min., the selectivity of the GaAs/photoresist etch is on the order of 2.3. Thus, a photoresist lens with a height of 29 µm after transferring into a GaAs, by etching, has a height of 72 µm (see Fig. 9).

The radius of the GaAs lens is 350 ± 20 µm and shows little deviation from the spherical profile, which is evident in Fig. 10 (note that the profile from profilometer is not to scale). The lens base diameter was reduced to 410 µm. The surface of the GaAs lens has average roughness R_a of about 25 ± 3 nm and maximum roughness R_s of about 290 ± 30 nm (see Fig. 11). The roughness was measured on the diameter of the lens after subtracting the profile matched to the shape of the lens and for flat fragments of the etched GaAs wafer, and both measurements were consistent.

The height of the lens after ICP etching was measured at the following points: (0, 0), (0, 6), (6, 6), (6, 0), (6, −6), (0, −6), (-6, −6), (-6, 0), and (−6, 6), as shown in Fig. 12 (left). The uniformity, which is defined as the deviation from the average lens height of the three manufacturing series, was 74.8 ± 1.5 µm, as presented in Fig. 12 (right).

The geometry of the experimentally obtained lens was recreated in OpticStudio using Freeform Z object to determine the plane of best focusing in the 0-36° angle of view. In Fig. 13, you can observe the lens geometry simulated in Optic Studio. It was calculated that the plane of best focusing should be 450 µm from the top of the lens, and this is how the lens was made on immersion detectors.

The immersion detectors were evaluated in terms of optical surface and angle of view. The optical surface was determined by measuring the full width at half maximum (FWHM) of the signal cross-section in the × and y axes, as shown in Fig. 14. The pixel size was calculated based on the measurement of a 0.1 × 0.1 mm^2 flat detector, presented in Fig. 14 (a). The physical size of the detector was previously measured using an optical microscope. The measurements reveal that the optical surface of the detector with the immersion lens forms a circle with a diameter of 330 ± 10 µm, and its angle of view is ± 20°, as shown in Fig. 15.

Current responsivity and IV characteristics were measured for flat detector and detector with immersion lens, both having physical area 0.1 × 0.1 mm^2 and illuminated through GaAs substrate. Their results are

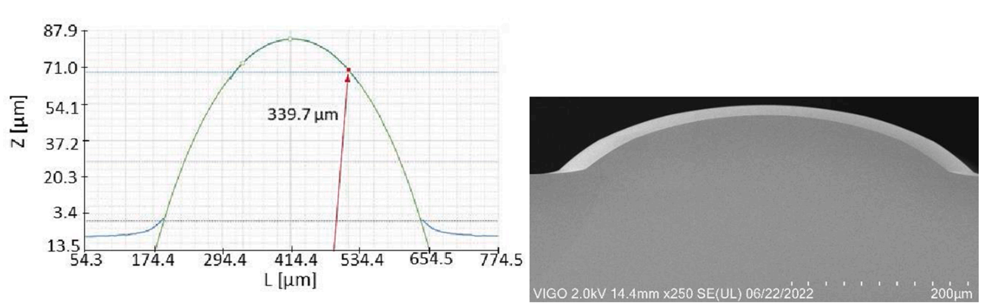

Fig. 10. A micro lens etched in GaAs: lens profile measured using optical profilometer (left) and SEM image of GaAs lens cross-section (right). In the left figure, the blue line is the surface profile, and the green line is the theoretical spherical profile. (For interpretation of the references to colour in this figure legend, the reader is referred to the web version of this article.)

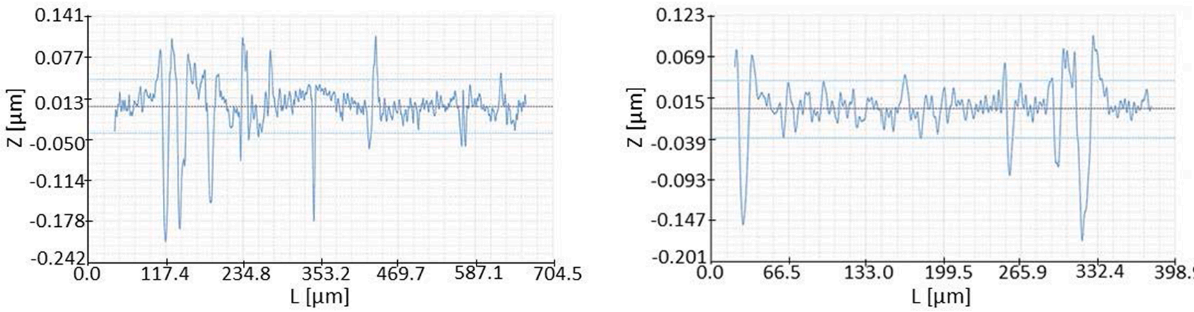

Fig. 11. Surface roughness of the GaAs lens (left), and the flat fragment of the GaAs surface after etching (right). Purple line is the mean value, blue line is RMS. (For interpretation of the references to colour in this figure legend, the reader is referred to the web version of this article.)

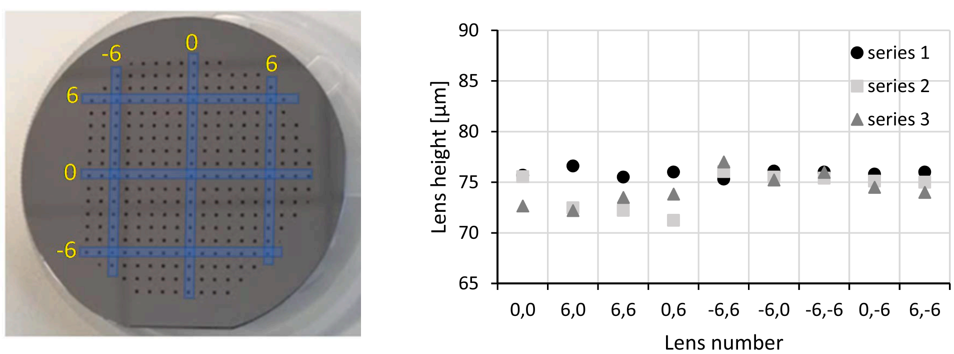

Fig. 12. The numbering of the lenses on the GaAs wafer (left) and the height of the individual lenses (right).

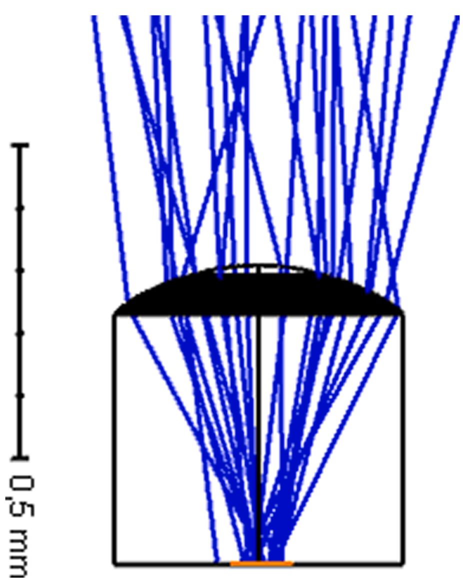

Fig. 13. Lens geometry simulated in OpticStudio.

presented in Fig. 16.

The detectors were measured without polarization, therefore, the current noise was Johnson-Niquist noise, defined as: $I_n = \sqrt{\frac{4k_B T \Delta f}{R}}$, where k_B is the Boltzmann constant, T is the temperature (in our case, 295 K), and R is the resistance [Ω]. In the calculations of R_i and D* of the detector with an immersion lens, the optical surface measured by the scanner was considered.

The electrical properties of the analyzed detectors are presented in Table 1. It can be observed that the resistance R, and current sensitivity R_i, are similar for both flat and immersed detectors, and they do not affect D*. Due to the immersion lens, the optical area of the detector increased by about 3 times, which resulted in an increase in D* from 1.15×10^9 cm•Hz$^{1/2}$/W for the flat 0.1 × 0.1 mm^2 detector to 3.49×10^9 cm•Hz$^{1/2}$/W for the immersed detector at 5µm.

The design presented for the microlens etched in GaAs stands out from previous studies in terms of lens diameter, and application. As shown in Table 2, lenses with a diameter of approximately 270–630 µm have already been produced in photoresist [9,11,12,15,16,18], but few of them were etched in the substrate. This work presents a process of simultaneously producing 280 lenses on the back side of the infrared photodetectors. While silicon has been the typical substrate material for photoresist microlenses [8,10,11,14,16,17], this work focuses on developing GaAs microlenses. Unlike polymer [19] and chalcogenide [20] lenses, GaAs is characterized by high and stable transmission and refractive index for infrared radiation [21]. In addition, this material is used as an epitaxial substrate in both HgCdTe and InAsSb-based detectors [21–23], therefore its application range is very wide. Most importantly, we integrated the microlens with the IR detector in our study, resulting in a three-fold increase in the detector's signal.

4. Summary

In this work, the parameters for the production of sub-millimeter base diameter immersion lenses in GaAs for group III-V infrared detectors were developed. The dimensions and their accuracy of the lenses on a 2'' wafer are 420 ± 20 µm in diameter and 78 ± 6 µm in height. The lenses have a clear aperture of 330 ± 10 µm. Lens fabrication does not cause degradation of the photosensitive structure, as reference flat detectors and detectors after the thermal reflow and dry etching process have the same resistances.

The field of view of the detector with immersion lens is 40° for the designed distance of the lens from the photosensitive structure and photosensitive size of 0.1 × 0.1 mm^2. Presented technique allows to

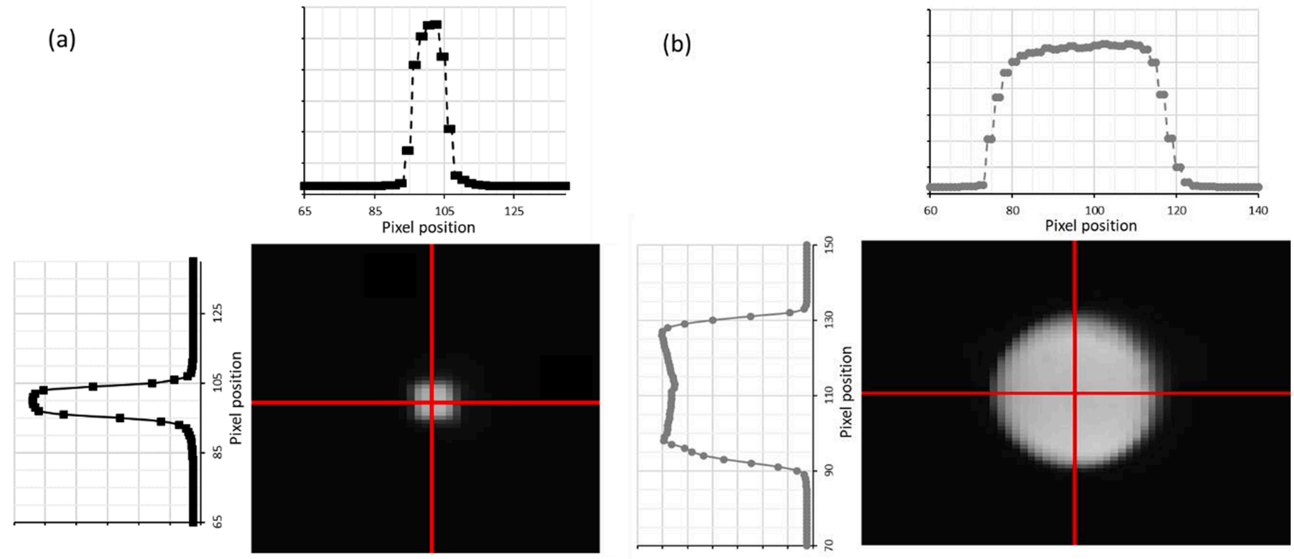

Fig. 14. Optical surface scan of (a) a flat detector with 0.1 × 0.1 mm^2 mesa, (b) detector with immersion lens and 0.1 × 0.1 mm^2 mesa. Distribution of intensity profiles from the detector in the cross-sectional view in × and y directions;

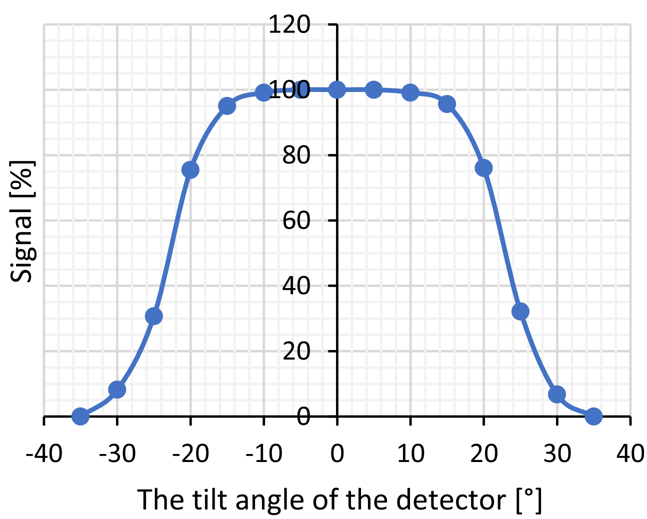

Fig. 15. The angle of view of the detector with immersion lens.

obtain uncooled detectors with improved detectivity and overcomes the problem of low resistance and signal to noise ratio (SNR) at room temperature. The use of an immersion lens resulted in increase of the detector detectivity D* by a factor three.

Table 1
Electrical parameters of detectors with an immersion lens and flat detectors with the same physical mesa surface. The flat detectors are marked “f” (f1, f2), and the detectors with an immersion micro lens are marked “i” (i1-i8).

Detector	R [Ω]	I_n [A/Hz$^{1/2}$]	R_i [A/W] at 5 μm	D*[cm*Hz$^{1/2}$/W] at 5 μm
i1	115	1.19E-11	1.28	3.31E + 09
i2	115	1.19E-11	1.34	3.48E + 09
i3	114	1.20E-11	1.35	3.48E + 09
i4	111	1.22E-11	1.39	3.54E + 09
i5	111	1.22E-11	1.45	3.67E + 09
i6	109	1.23E-11	1.36	3.41E + 09
i7	121	1.16E-11	1.34	3.57E + 09
i8	119	1.17E-11	1.33	3.48E + 09
f1	117	1.19E-11	1.48	1.25E + 09
f2	118	1.18E-11	1.23	1.04E + 09

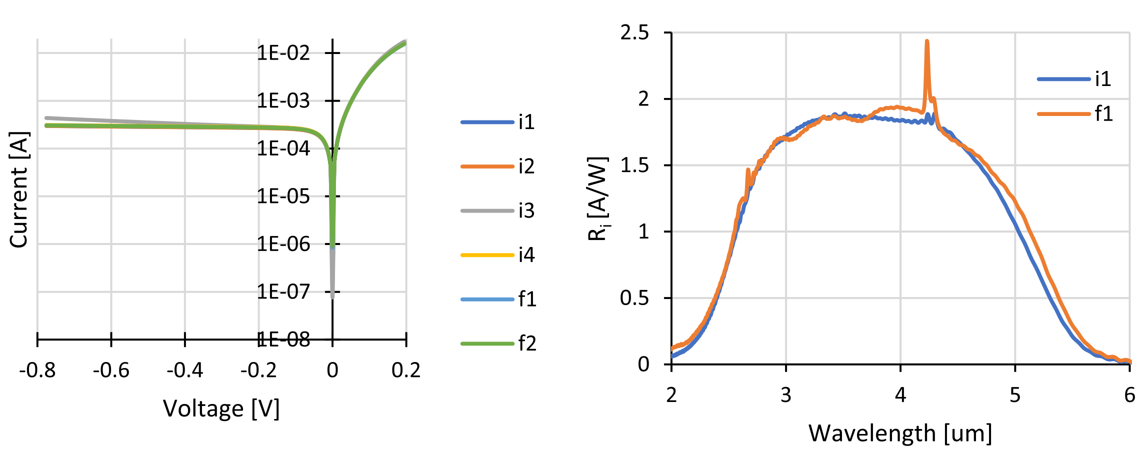

Fig. 16. IV characteristics (left) and current responsivity R_i (right). The flat detector marked f and the detector with immersion lens marked i.

Table 2
A review of the literature on the manufacture of microlenses. Publications in which a technique other than thermal reflow was used are marked with a gray background.

Ref.	Technology	Photoresist and its thickness	Photoresist microlens design	ICP-RIE gas mixture	Substrate material and the microlens design after etching	Application
[8]	Reflow at 170–250 °C for 30 sec.		height 0.4 µm diameter 3.5 µm	not applicable	silicon	
[9]	Reflow at 150–200 °C		1. height 13 µm1. diameter 145 µm2. height 70 µm2. diameter 1 mm	not stated	fused silica/1. height 20 µm1. diameter 190 µm2. height 11 µm2. diameter 145 µm	
[10]	Reflow at 120–160 °C	ma-P 1275	height 7–9 µm diameter 16, 20, 24 and 28 µm	not applicable	silicon with surface modification	
[11]	Gray scale mask	thickness 2.6 µm	height 2.4 µm diameter 460 µm	SF_6: O_2 = 160:90 sccm	silicon/ height 46 µm diameter 480 µm	IR sensor, micro lens causes 4.2x signal increase
[12]	Reflow at 140 °C for 3 min	AZ4620 / thickness 16 µm,	thickness ~ 15–26 µm diameter 630 µm	not applicable	glass	
[14]	Reflow at 140 °C for 20 min	SPR220 7.0	height 7 µm diameter 38 µm	O_2: SF_2 = 20:25 sccm	silicon height 2.2 µm diameter 38 µm	
[15]	Reflow at 160 °C for 6 min	AZ 1518/ thickness 1 µm and AZ 4620 A/ thickness 11 µm	height um and diameter 272 um	not applicable	glass	
[16]	Reflow at 145 °C	AZ 4562/ thickness 11.5 µm	height um and diameter 270 um	SF_6 and O_2	silicon	fiber to fiber coupling
[17]	Nanoimprint litography followed by reflow at 180–220 °C for 10–20 min	Polystyrene/ thickness 7.8, 4.2, 1.9 µm;	diameter 25 µm	not applicable	silicon	
[18]	Reflow at 95 °C for 1 h + micro-molding	SU-8/ thickness 1 mm	meniscus lens diameter 500 µm	not applicable	PDMS (poly-dimethylsiloxane) height 98–139 µm diameter 300, 500 um;	

Funding

This work was supported by National Centre for Research and Development (NCBR) grant No. TECHMATSTRATEGIII/0026/2019 and MAZOWSZE/0090/19–00.

Declaration of Competing Interest

The authors declare that they have no known competing financial interests or personal relationships that could have appeared to influence the work reported in this paper.

Data availability

Data will be made available on request.

References

[1] J. R. Brag, A. M. Shulenberger, US Patent, patent no. USOO5877500A, 1999.
[2] S.F. Pellicori, H.P. Wurtz, Optical crosstalk in infrared detector arrays, SPIE 124 (1977) 69–76.
[3] H.R. Hardaway, C.T. Elliott, N.T. Gordon, J. Crowder, Optical immersion of mid-infrared LEDs and photodiodes for gas sensing applications, Proc. SPIE 4947 (2003).
[4] J. Piotrowski, Optical immersion of IR photodetectors as an effective way to reduce cooling requirements, Opt. Appl. XXIII (1) (1993).
[5] M.A. Remennyi, N.V. Zotova, S.A. Karandashev, B.A. Matveev, N.M. Stus', G. N. Talalakin, Low voltage episode down bonded mid-IR diode optopairs for gas sensing in the 3.3-4.3 µm spectral range, Sens. Actuators B-Chemical 91 (1–3) (2003) 256–261.
[6] M.A. Remennyi, B.A. Matveev, N.V. Zotova, S.A. Karandashev, N.M. Stus, N. D. Ilinskaya, InAs and InAs(Sb)(P)(3–5 &mgr;m) immersion lens photodiodes for portable optic sensors, Proc. SPIE 658504 (2007).
[7] G.Y. Sotnikova, G.A. Gavrilov, S.E. Aleksandrov, A.A. Kapralov, S.A. Karandashev, B.A. Matveev, M.A. Remennyy, Low voltage CO_2-gas sensors based on III-V Mid-IR immersion lens diode optopairs: where we are and how far we can go? IEEE Sens. J. 10 (2) (2010).
[8] S. Audran, B. Faure, B. Mortini, C. Aumont, R. Tiron, C. Zinck, Y. Sanchez, C. Fellous, J. Regolini, J.P. Reynard, G. Schlatter, G. Hadzzoannou, Study of dynamical formation and shape of microlenses formed by the reflow method, Proc. of SPIE 61534D–1 (2006).
[9] P.h. Nussbaum, R. Völkel, H.P. Herzig, M. Eisner, S. Haselbeck, Design, fabrication and testing of microlens arrays for sensors and microsystems, Pure Appl. Opt. 6 (1997) 617–636.
[10] D. Jucius, V. Grigaliunas, A. Lazauskas, E. Sapeliauskas, B. Abakeviciene, S. Smetona, S. Tamulevicius, Effect of fused silica surface wettability on thermal reflow of polymer microlens arrays, Microsyst Technol 23 (2017) 2193–2206.
[11] R. Yamazaki, A. Obana, M. Kimata, Microlens for uncooled infrared array sensors, Electron. Commun. Jpn. 96 (2) (2013).
[12] S.i. Di, D.u. Ru-xu, The cotrolling of microlens contour by adjusting developing time in thermal reflow method, Proc. of SPIE 7381D–1 (2009).
[13] R. Amarit, A. Kopwitthaya, P. Pongsoon, U. Jarujareet, K. Chaitavon, S. Porntheeraphat, S. Sumriddetchkajorn, High-quality large-magnification polymer lens from needle moving technique and thermal assisted moldless fabrication process, PLoS One 11 (1) (2016) e0146414.
[14] Y. Zhang, Y. Li, L. Liu, C. Yang, Y. Chen, S. Yu, Demonstration of diamond microlens structures by a three-dimensional (3D) dual-mask method, Opt. Express 25 (13) (2017).
[15] S. Haselbeck, H. Schreiber, J. Schwider, N. Streibl, Microlens fabricated by melting a photoresist on a base layer, Opt. Eng. 32 (2) (1993) 1322–1324.
[16] N. Mangal, B. Snyder, J. Van Campenhout, G. Van Steenberge, J. Missinne, Monolithic integration of microlenses on the backside of a silicon photonics chip for expanded beam coupling, Opt. Express 29 (5) (2021) 7601–7615.
[17] S.G. Heo, D. Jang, H.-J. Koo, H. Yoon, Large-area fabrication of microlens arrays by using self-pinning effects during the thermal reflow process, Opt. Express 27 (3) (2019) 3439–3447.
[18] J.Y. Tan, G. Goh, J. Kin, Microfabrication of microlens by timed-development-and-thermal-reflow (TDTR) process for projection litography, Micromachines 11 (3) (2020) 277.
[19] M.G. Han, Y.J. Park, S.H. Kim, B.S. Yoo, H.H. Park, Thermal and chemical stability of reflowed-photoresist microlenses, J. Micromech. Microeng. 14 (2004) 398–402.
[20] K.H. Nam, A. Lee, S.K. Lee, K. Hur, H. Han, Infrared transmitting polyimides based on chalcogenide element-blocks with tunable high-refractive indices and broad optical windows, J. Mater. Chem. C 34 (2019).
[21] T. Skauli, P.S. Kuo, K.L. Vodopyanov, T.J. Pinguet, O. Levi, L.A. Eyres, J.S. Harris, M.M. Fejer, B. Gerard, L. Becouarn, E. Lallier, Improved dispersion relations for GaAs and applications to nonlinear optics, J. Appl. Phys. 94 (2003) 6447–6455.
[22] K. Michalczewski, Ł. Kubiszyn, P. Martyniuk, C.H. Wu, J. Jureńczyk, K. Grodecki, D. Benyahia, A. Rogalski, J. Piotrowski, Demonstration of HOT LWIR T2SLs InAs/InAsSb photodetectors grown on GaAs substrate, Infrared Phys. Technol. 95 (2018) 222–226.
[23] W. Gawron, J. Sobieski, T. Manyk, M. Kopytko, P. Madejczyk, J. Rutkowski, MOCVD Grown HgCdTe Heterostructures for Medium Wave Infrared Detectors, Coatings 11 (5) (2021) 611.